

## Porosity Analysis of *Acacia catechu* Seed-derived Carbon Materials Activated with Sodium Hydroxide and Potassium Hydroxide: Insights from Methylene Blue and Iodine Number Methods

Pawan Kumar Mishra<sup>1,2,3</sup>, Sabin Aryal<sup>2</sup>, Hari Bhakta Oli<sup>2</sup>, Timila Shrestha<sup>2</sup>, Dharendra Jha<sup>2</sup>, Ram Lal (Swagat) Shrestha<sup>2\*</sup>, Deval Prasad Bhattarai<sup>2\*</sup>

<sup>1</sup> Department of Chemistry, Tri-Chandra Multiple Campus, T.U., Kathmandu, Nepal

<sup>2</sup> Department of Chemistry, Amrit Campus, T.U., Kathmandu, Nepal

<sup>3</sup> Central Department of Chemistry, Kirtipur, T.U., Kathmandu Nepal

\*Corresponding E-mail: [swagatstha@gmail.com](mailto:swagatstha@gmail.com), [deval.bhattarai@ac.tu.edu.np](mailto:deval.bhattarai@ac.tu.edu.np)

(Received: December 8, 2024; revised: December 30, 2024; accepted: January 5, 2025)

### Abstract

The significant adsorption capacity of activated carbon makes it a highly effective adsorbent material. The choice of activating chemicals plays a crucial role in determining the surface morphology and pore size distribution of the resulting activated carbon. In this study, potassium hydroxide and sodium hydroxide were employed as chemical activating agents in the preparation of activated carbon from the waste biomass of *Acacia catechu* seeds through a carbonization process. Fourier-transform infrared spectroscopy (FTIR) was utilized to examine the surface functional groups, while X-ray diffraction (XRD) analysis provided insights into the crystallinity of the activated carbons. Field-Emission Scanning Electron Microscopy (FESEM) was employed to analyze surface morphology. For the adsorption capacity assessment, methylene blue number (MBN) and iodine number (IN) method were employed. The activated carbon derived using KOH-activator (ACSK-6) exhibited higher iodine number (1269.62 mg/g) and methylene blue number (238.62 mg/g) compared to activated carbon synthesized using NaOH (ACSN-6). The well-developed porosity and superior adsorption capacity of the ACSK-6 sample underscore its potential in various application.

**Keywords:** Activated carbon, *Acacia catechu*, Activating agent, MB number, IN number

### Introduction

The astonishing capabilities of activated carbons as adsorbents have led to a growing interest in potential application in various field. These materials' large surface area, micro-porous assembly, and notably high degree of surface responsiveness are responsible for adsorptive properties. The porous structure of activated carbons plays a major role in their adsorptive properties and its efficacy. Generally, these materials are produced from precursors with high carbon content [1]. The intrinsic properties of activated carbon materials are

fundamentally influenced by the selection of precursors, choice of activating agent, carbonization temperature and the specific methodologies employed during their synthesis [2], [3]. The thermal conditions govern the structural transformation, pore development, and surface area characteristics of the material, while the adopted preparation techniques dictate the chemical composition, functional group distribution, and overall adsorption capacity [4], [5]. High-temperature carbonization is essential for generating porous activated carbon, as elevated temperature cause

volatile organic matters to escape from the carbon matrix, creating porous surface [6], [7], [8].

The activated carbon produced from different sources like agriculture waste and renewable biomass are economic as well as environmentally friendly which ultimately helps to reduce the reliance on the fossil fuels [9]. The viability of creating high-quality activated carbon, the availability and affordability of the raw materials, and the materials' storage lifespan are pre-requisite condition for selecting an ideal precursor material [10]. There are two main approaches of generating activated carbons, (i) physical activation and (ii) chemical activation method [11], [12], [13]. Amid these, activation by chemical method precedence physical method in the sense that it requires relatively lower temperature for producing highly porous activated carbon [1].

Among various biomass-derived precursors, the seeds of *Acacia catechu* hold significant potential as a valuable resource for synthesizing nanoporous activated carbon [14]. The high lignocellulosic content, comprising cellulose, hemicellulose, and lignin, in *Acacia catechu* seeds renders them particularly suitable for carbonization and activation processes [15]. These constituents contribute to the formation of a robust carbonaceous framework with well-developed porosity, making the material ideal for diverse applications such as adsorption, catalysis, and energy storage [14].

To the finest of our knowledge, a little exploration has been done on how activating chemicals plays crucial role on the ability of activated carbons made from *Acacia catechu* seeds to perform adsorption process and the distribution of the pore in the surface. In this work, iodine and methylene blue number methods were employed to quantitatively evaluate the microporous and mesoporous

nature of the synthesized material. The aim of this study was the inherent biomass of *Acacia catechu* seeds, which demonstrated exceptional adsorptive properties. Finally, *Acacia catechu* seeds showed exceptional high methylene blue and iodine adsorptive capabilities by KOH activating agent than NaOH.

## Materials and Methods

### Collection and Pre-carbonization of Precursor

The *Acacia catechu* seeds were obtained in June of 2021 from the Garambesi region, Rainas-7, Lumjung district, Nepal. The collected seeds were subjected to shade-drying for a three-month. The dried substance was ground into a fine powder using Herbal Disintegrator (FW 177) at Amrit Campus. The material was then subjected to pre-carbonization process. Specifically, 60 g of previously ground seed material was placed in a muffle furnace for pyrolysis at 300 °C for three hours. The pre-carbonized materials derived from *Acacia catechu* seed is labeled as ACSP-0.

### Activation of the materials

The preparation process began by accurately mixing 10 g of pre-carbonized *Acacia catechu* seed powder with an equimolar quantity of potassium hydroxide (KOH) and sodium hydroxide (NaOH), separately. The mixture was ground into a fine paste using an agate mortar and pestle for two hours to ensure uniformity. It was then transferred into a ceramic boat and left to stabilize at room temperature for 24 hours. Subsequently, the material was subjected to heat treatment at 600 °C under a nitrogen atmosphere. The resulting activated carbon was neutralized with 1M hydrochloric acid (HCl) followed by repeated washing with distilled water. As-prepared activated carbon (AC) was dried in a hot air oven at 80 °C for eight hours, followed by a vacuum drying for six hours to remove any residual moisture. The dried AC was

agitated into a fine powder using an agate mortar, producing activated carbon suitable for further characterization. The activated carbon derived at temperature of 600 °C using chemical activators KOH and NaOH were labeled as ACSK-6 and ACSN-6, respectively.

### Iodine Number (IN)

The micro-porosity of the activated carbon materials was evaluated by determining the iodine number (IN). For this analysis, a 1 g of carbonaceous material (ACSP-0, ACSK-6 and ACSN-6) were added to each of three conical flasks containing 5 mL of 5% hydrochloric acid (HCl). The samples were meticulously soaked by the acid through swirling, and the solution was then boiled and cooled to room temperature. Later, 10 mL of 0.1 N iodine solution was added to each flask, and the solution was shaken for 15 minutes using a shaker at 200 RPM. After allowing the solution to settle, it was filtered using filter paper. The filtrate was titrated against standardized 0.1 N sodium thiosulphate solution. A few drops of freshly prepared starch indicator were added when the solution turned straw yellow, resulting in a dark blue color. The titration continued until the solution became colorless. The iodine number was calculated using the following formula:

$$\text{Iodine Number} = \frac{\text{Amount of I}_2 \text{ in mg adsorbed by AC}}{\text{Weight of AC taken in g}}$$

$$O \frac{x}{m} = \frac{[(126.93 N_1 V_1) - \left(\frac{V_1 + V_{\text{HCl}}}{V_F}\right) \times (126.93 N_2 V_2)]}{M_C} \dots (1)$$

Here,  $N_1$  = Normality of iodine solution,  $V_1$  = Volume of iodine solution,  $V_{\text{HCl}}$  = Added volume of 5% HCl,  $V_F$  = Filtrate volume used in titration,  $N_2$  = Normality of sodium thiosulfate solution,  $V_2$  = Consumed volume of sodium thiosulfate solution and,  $M_C$  = Mass of activated carbon,  $\frac{x}{m}$  = iodine absorbed per gram of carbon, (mg/g).

### Methylene Blue Number (MBN)

The adsorption capacity of activated carbon was evaluated using the methylene blue adsorption technique through batch adsorption experiments. Herein, 0.1 g sample of carbonaceous materials (ACSP-0, ACSK-6 and ACSN-6) were treated with 75 mL of a methylene blue solution of 100 ppm concentration. The mixture was agitated at 200 RPM for 4.5 hours using a shaker at 25 °C, followed by a 24-hour equilibration period. Afterward, the solution was filtered through Whatman filter paper (No. 42), and the residual methylene blue concentration in the filtrate was measured with a spectrophotometer (Labtronics, LT-2802). The amount of methylene blue adsorbed ( $q_t$ ), expressed in milligrams per gram of adsorbent (mg/g) at a specific time (t), was calculated using the following formula:

$$MBN = \frac{(C_0 - C_e)V}{W} \dots (2)$$

Where,  $C_0$  and  $C_e$  are the initial and equilibrium concentrations of methylene blue solution in milligrams per liter (mg/L or ppm), respectively.  $W$  represents the mass of the adsorbent in grams (g), and  $V$  is the volume of the solution in liters (L).

## Results and Discussion

### Study of functional group

Functional group present in the carbonaceous material was studied in terms of Fourier Transform Infra-red (FTIR) spectroscopy. The surface characteristics and adsorption capabilities of activated carbons are significantly affected by the existence of oxygen-containing surface functional groups [16]. The FTIR spectra of as prepared activated carbon samples are depicted in **Fig. 1**. The FTIR spectra of all the samples demonstrate notable similarity despite being produced using different activating agents. Prominent bands are observed in wavenumber between 800-1700  $\text{cm}^{-1}$

<sup>1</sup> [17]. The band around  $1700\text{ cm}^{-1}$  corresponds to the stretching vibrations of  $\text{-C=O}$  bonds, indicative of carbonyl groups presents in the activated carbon derived from *Acacia catechu* seeds. Similarly, the strong band at  $1425\text{ cm}^{-1}$  is attributed to the stretching vibrations of C-C bonds, while the band observed at approximately  $1600\text{ cm}^{-1}$  suggests stretching vibrations of highly conjugated carbonyl groups ( $\text{C=O}$ ) associated with aromatic ring systems [18]. The absorption bands between  $1100$  and  $1200\text{ cm}^{-1}$  signify C-O bond stretching, and the weak band slightly above  $3000\text{ cm}^{-1}$  across all samples points to unsaturated alkenyl  $\text{C=C}$  stretching vibrations. Additionally, the bands in the  $860\text{--}600\text{ cm}^{-1}$  range denote aromatic C-H bending vibrations [19]. A weak vibration band near  $3740\text{ cm}^{-1}$  is associated with the O-H bond stretching vibrations of phenol or alcohol groups [20]. The FTIR spectra indicates the presence of residual oxygenated surface functional groups, such as lactones, carboxyls, carbonyls, and hydroxyls, in all activated carbon samples [21].

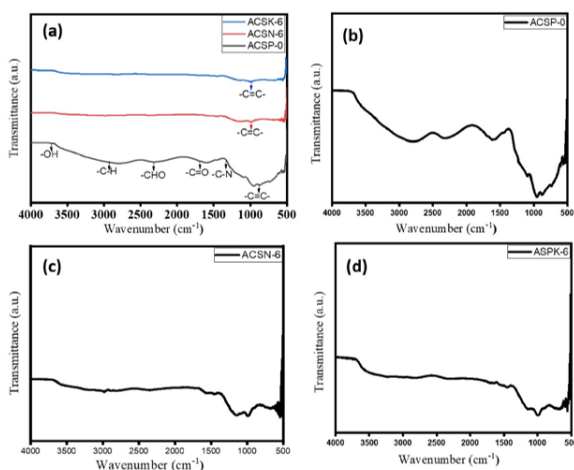


**Fig. 1:** FTIR spectra of various carbonaceous materials (ACSP-0, ACSK-6 and ACSN-6).

### X-ray diffraction (XRD) characterization

The structural purity and crystallinity of KOH-activated carbon and NaOH-activated carbon were evaluated using X-ray diffraction (XRD) analysis. The diffraction patterns

demonstrated the phase purity of the samples, characterized by broad peaks typical of carbon materials, with no evidence of residual activating agents, confirming the synthesis of pure activated carbon. XRD patterns for ACSP-0, ACSN-6, and ACSK-6, recorded over a  $2\theta$  range of  $10^\circ$  to  $90^\circ$ , are presented in **Fig. 2**. Notably, all samples displayed broad and sharp XRD pattern, including a prominent broad peak at  $2\theta \approx 24.6^\circ$ , corresponding to a d-spacing value of approximately  $0.33\text{ nm}$  and the (002) plane, indicative of the graphitic structure of the carbon materials. Additionally, a smaller peak observed at  $2\theta \approx 43.7^\circ$  further corroborates the carbonaceous nature of the samples, consistent with prior studies [22].

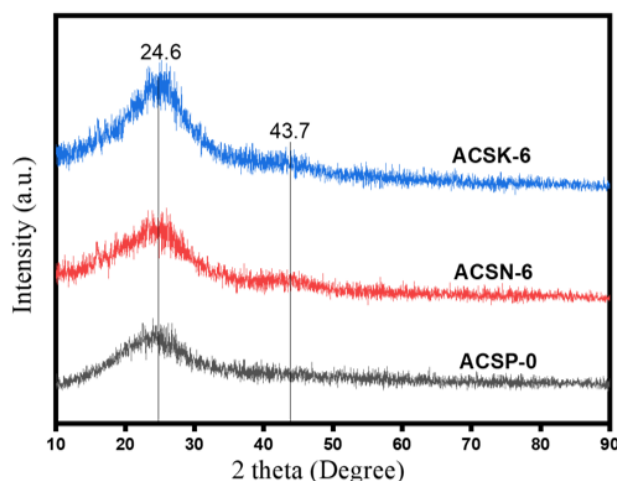


**Fig. 2:** XRD of Pre-carbonized sample, carbonization with NaOH and carbonization with KOH.

### Iodine and methylene blue number

The performance of activated carbon is commonly evaluated using methylene blue (MB) and iodine (I) adsorption methods, as they provide valuable insights into pore size and structure. Iodine adsorption assesses the capacity to adsorb smaller molecules due to iodine's small molecular size [23]. In contrast, methylene blue number primarily measures molecules with mesoporous size [24]. The iodine number value of the sample is illustrated in the bar-graph, **Fig. 3 (a)**. The sample activated at

600 °C using KOH (ACSK-6) exhibits the highest iodine number value of 1269.62 mg/g as compared to NaOH activated carbon at the same temperature (972.71 mg/g). It is clear that the micropore development within the surface of the as prepared activated carbon not only depend upon activation temperature. The activating agent employed for activation and their specific action also plays crucial role.

Similarly, the methylene blue number (MBN) was determined by measuring the change in methylene blue concentration before and after adsorption by the as-prepared AC. The absorbance was measured using spectrophotometer. The methylene blue number values indicate the mesopore content in the activated carbon [25], [26]. The maximum wavelength for the solution was observed by taking the absorbance within the wavelength of visible range (500-800 nm). The wavelength at which maximum absorbance of MB solution observed was found to be 665 nm. The methylene blue adsorption value for the KOH-activated carbon sample (ACSK-6) is higher (238.62 mg/g) compared to ACSN-6 (185.12 mg/g) and ACSP-0 (94.60 mg/g), as shown in **Fig. (b)**. The higher value of the MBN suggests the presence of high number of mesopores within the carbon matrix. Among the tested samples, the adsorption capabilities of iodine and methylene blue follow the order: ACSK-6 >ACSN-6 >ACSP-0. Higher temperatures generally enhance the removal of volatile components from the precursor material and facilitate the opening of pores. At the meantime, activating agents react with the chemical contents of the precursor and produce gases like CO, CO<sub>2</sub> [27]. The development of micropores and mesopores is higher in KOH-activated carbon compared to NaOH-activated carbon due to the greater chemical reactivity of KOH, which

facilitates deeper penetration into the carbon matrix and promotes more effective gasification reactions [28]. KOH forms highly reactive intermediates, such as potassium carbonate and metallic potassium, which catalyzes the formation of pores more efficiently than sodium-based intermediates [29], [30]. Additionally, the smaller ionic radius and better mobility of potassium ions allow for uniform pore distribution and greater structural expansion of the carbon framework. KOH activation also occurs within an optimal temperature range (600–800°C), enhancing gas evolution and pore development [30]. These factors collectively result in a higher surface area and greater microporosity and mesoporosity in KOH-activated carbon compared to NaOH-activated carbon [31].

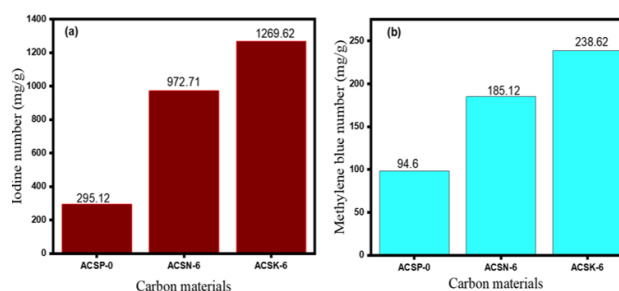


**Fig. 3:** Bar graph demonstrating (a) iodine number and (b) methylene blue number of samples (ACSP-0, ACSN-6 and ACSK-6).

### Field Emission Scanning Electron Microscopy (FESEM)

The morphological structure of the carbon materials was examined by FESEM. **Fig. 4 (a-c)** depicts the FESEM image of ACSP-0, ACSN-6, and ACSK-6 at magnification of 100 nm. These images highlight the significant influence of activating agents on the surface topology and porosity of the carbon samples. The pre-carbonized char, shown in **Fig. 4 (a)**, features a relatively smooth surface with minimal porosity, indicating that the sample almost devoid of porous nature. The NaOH-activated carbon in



**Fig. 4 (b)** shows a distribution of small and uneven pores across its surface, suggesting a moderate level of activation [32]. In contrast, the KOH-activated carbon, illustrated in **Fig. 4 (c)**, exhibits a highly porous interconnected structure compared to others, indicating a higher degree of activation and pore development. However, the pore distribution is not entirely uniform, reflecting the localized nature of the activation process. The differences in pore structures between NaOH and KOH activation highlight their distinct mechanisms [31]. The KOH activation involves structural breakdown by etching the carbon surface followed by gasification of the lignocellulosic contents that escape out from carbon matrix, leaving behind a porous structure [33]. In comparison, NaOH activation promotes a less intensive reaction, resulting in smaller and less developed pores [34].

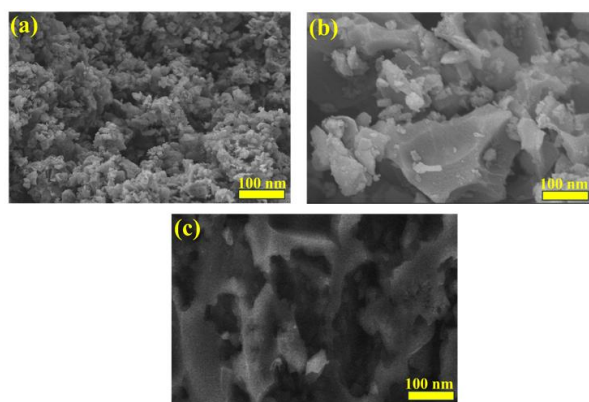


**Fig. 4:** Morphological study: FESEM image of (a) ACSP-0 (b) ACSN-6, and (c) ACSK-6, respectively.

## Conclusions

This study investigated the potential of utilizing waste *Acacia catechu* seeds to produce nanoporous activated carbon through a simple chemical activation method, using KOH and NaOH as activating agents independently at 600°C. The carbonaceous materials as prepared were characterized using FTIR, XRD, FESEM, iodine number and methylene blue number analysis. This study highlights the critical role

of KOH in producing activated carbon (ACSK-6) with well-developed porosity, which is attributed to its high reactivity, efficient ion diffusion, and catalytic gasification effects exhibiting higher iodine and methylene blue number of 1269.62 mg/g and 238.62 mg/g, respectively compared to other samples (ACSN-6 and ACSP-0). This finding is also consistent with the FESEM analysis. These studies confirmed the superior adsorption capacity of KOH-activated carbon compared to its NaOH-activated counterpart. Overall, the lignocellulosic contents prevalent in *Acacia catechu* seeds makes them an excellent precursor for activated carbon production, and the use of KOH not only enhances pore formation but also ensures economic feasibility, making it a preferred choice for industrial applications as an efficient adsorbent material.

## Acknowledgements

The authors are grateful for the support provided by the University Grant Commission (UGC) under Grant No. PhD S&T-04.

## Author's Contribution Statement

**Pawan Kumar Mishra:** Investigation, Methodology, Formal analysis, Writing: original manuscript, **Hari Bhakta Oli:** Formal analysis, **Sabin Aryal:** Investigation, Methodology, Writing: review and editing, **Timila Shrestha:** Investigation, Writing: review and editing, **Dhirendra Jha:** Formal analysis, **Ram Lal (Swagat) Shrestha:** Conceptualization, Supervision, Analyzing data and Writing: review and editing, **Deval Prasad Bhattarai:** Conceptualization, Supervision, Analyzing data and Writing: review and editing,

## Conflict of Interest

The authors do not have any conflict of interest throughout this research work.

## Data Availability Statement

The data supporting this study's findings are available from the corresponding authors upon reasonable request.

## References

1. F. T., Ademiluyi, & E. O., David-West, "Effect of chemical activation on the adsorption of heavy metals using activated carbons from waste materials", *International Scholarly Research Notices*, **2012** (1), 674209. <https://doi.org/10.5402/2012/674209>
2. B. Bestani, N. Benderdouche, B. Benstaali, M. Belhakem, and A. Addou, "Methylene blue and iodine adsorption onto an activated desert plant", *Bioresource technology*, 2008, **99**(17), 8441-8444. <https://doi.org/10.1016/j.biortech.2008.02.053>
3. P. L. M., Langama, J. J., Anguile, C., Bissielou, A., Bouraïma, A. N. M. M., Ndong, D., Kouotou, & J. K., Mbadcam, "Preparation and characterization of activated carbons from Asparagus palm (*Laccosperma robustum*) bark by chemical activation with H<sub>3</sub>PO<sub>4</sub> and KOH", *American Journal of Analytical Chemistry*, 2023, **14**(2), 55-71. <https://doi.org/10.4236/ajac.2023.142004>
4. W. M. Lewandowski, M. Ryms, and W. Kosakowski, "Thermal biomass conversion: A review", *Processes*, 2020, **8**(5), 516. <https://doi.org/10.3390/pr8050516>
5. Y. Huang, E. Ma, and G. Zhao, "Thermal and structure analysis on reaction mechanisms during the preparation of activated carbon fibers by KOH activation from liquefied wood-based fibers", *Industrial Crops and Products*, 2015, **69**, 447-455. <https://doi.org/10.1016/j.indcrop.2015.03.002>
6. K. Ö. Köse, B. Pişkin, and M. K. Aydınol, "Chemical and structural optimization of ZnCl<sub>2</sub> activated carbons via high temperature CO<sub>2</sub> treatment for EDLC applications", *International Journal of Hydrogen Energy*, 2018, **43**(40), 18607-18616. <https://doi.org/10.1016/j.ijhydene.2018.03.222>
7. W. M. A. W. Daud, W. S. W. Ali, and M. Z. Sulaiman, "Effect of activation temperature on pore development in activated carbon produced from palm shell", *Journal of Chemical Technology & Biotechnology: International Research in Process, Environmental & Clean Technology*, 2003, **78**(1), 1-5. <https://doi.org/10.1002/jctb.712>
8. R. Shokrani Havigh and H. Mahmoudi Chenari, "A comprehensive study on the effect of carbonization temperature on the physical and chemical properties of carbon fibers", *Scientific Reports*, 2022, **12**(1), 10704. <https://doi.org/10.1038/s41598-022-15085-x>
9. U. Itodo, F. W. Abdulrahman, L. G. Hassan, S. a Maigandi, and H. U. Itodo, "Application of methylene blue and iodine adsorption in the measurement of specific surface area by four acid and salt treated activated carbons", *New York science journal*, 2010, **3**(5), 25-33. <https://doi.org/10.4314/ijonas.v5i1.49950>
10. R. Rajbhandari, L. K. Shrestha, and R. R. Pradhananga, "Nanoporous activated carbon derived from Lapsi (*Choerospondias Axillaris*) seed stone for the removal of arsenic from water", *Journal of nanoscience and nanotechnology*, 2012, **12**(9), 7002-7009. <https://doi.org/10.1166/jnn.2012.6568>
11. O. Das and A. K. Sarmah, "Mechanism of waste biomass pyrolysis: Effect of physical and chemical pre-treatments", *Science of the Total Environment*, 2015, **537**, 323-334. <https://doi.org/10.1016/j.scitotenv.2015.07.076>
12. J. Pallarés, A. González-Cencerrado, and I. Arauzo, "Production and characterization of activated carbon from barley straw by physical activation with carbon dioxide and steam", *Biomass and bioenergy*, 2018, **115**, 64-73. <https://doi.org/10.1016/j.biombioe.2018.04.015>
13. S. K. Shahcheragh, M. M. Bagheri Mohagheghi, and A. Shirpay, "Effect of physical and chemical activation methods on the structure, optical absorbance, band gap and urbach energy of porous activated carbon", *SN Applied Sciences*, 2023, **5**(12), 313.

- <https://doi.org/10.1007/s42452-023-05559-6>
14. P. K., Mishra, K. R., Shrestha, H. B., Oli, T., Shrestha, L. P., Joshi, R. L. S., Shrestha, & D. P., Bhattarai, High-performance porous activated carbon derived from Acacia catechu bark as nanoarchitectonics material for supercapacitor applications, *Journal of the Taiwan Institute of Chemical Engineers*, 2024, **165**, 105761. <https://doi.org/10.1016/j.jtice.2024.105761>
  15. K. Lakshmikandhan and A. Ramadevi, "Removal of lead in water using activated carbon prepared from *Acacia catechu*", *Water SA*, 2019, **45**(3), 374-382. <https://doi.org/10.17159/wsa/2019.v45.i3.6734>
  16. D. Setyaningrum and A. Rohman, "Analysis of corn and soybean oils in red fruit oil using FTIR spectroscopy in combination with partial least square", *International Food Research Journal*, 2013, **20**(4), 1977. <https://www.researchgate.net/publication/289549866>
  17. M. Danish and T. Ahmad, "A review on utilization of wood biomass as a sustainable precursor for activated carbon production and application", *Renewable and Sustainable Energy Reviews*, 2018, **87**, 1-21. <https://doi.org/10.1016/j.rser.2018.02.003>
  18. Y. Fan, P. Liu, B. Zhu, S. Chen, K. Yao, and R. Han, "Microporous carbon derived from acacia gum with tuned porosity for high-performance electrochemical capacitors", *International Journal of Hydrogen Energy*, 2015, **40**(18), 6188-6196. <https://doi.org/10.1016/j.ijhydene.2015.03.090>
  19. D. Kumar, C. L. Thakur, and D. R. Bhardwaj, "Biodiversity conservation and carbon storage of *Acacia catechu* Willd. dominated northern tropical dry deciduous forest ecosystems in north-western Himalaya: Implications of different forest management regimes", *Frontiers in Environmental Science*, 2022, **10**, 981608. <https://doi.org/10.3389/fenvs.2022.981608>
  20. R. Ali, Z. Aslam, R. A. Shawabkeh, A. Asghar, and I. A. Hussein, "BET, FTIR, and RAMAN characterizations of activated carbon from waste oil fly ash", *Turkish journal of chemistry*, 2020, **44**(2), 279-295. <https://doi.org/10.3906/kim-1909-20>
  21. S., Jiao, Y., Yao, J., Zhang, L., Zhang, C., Li, H., Zhang, ... & J., Jiang, "Nano-flower-like porous carbon derived from soybean straw for efficient NS co-doped supercapacitors by coupling in-situ heteroatom doping with green activation method", *Applied Surface Science*, 2023, **615**, 156365. <https://doi.org/10.3906/kim-1909-20>
  22. P. González-García, "Activated carbon from lignocellulosics precursors: A review of the synthesis methods, characterization techniques and applications", *Renewable and Sustainable Energy Reviews*, **82**, 1393-1414. <https://doi.org/10.1016/j.rser.2017.04.117>
  23. B. Bestani, N. Benderdouche, B. Benstaali, M. Belhakem, and A. Addou, "Methylene blue and iodine adsorption onto an activated desert plant", *Bioresource technology*, 2008, **99**(17), 8441-8444. <https://doi.org/10.1016/j.biortech.2008.02.053>
  24. C. A. Nunes and M. C. Guerreiro, "Estimation of surface area and pore volume of activated carbons by methylene blue and iodine numbers", *Química Nova*, 2011, **34**, 472-476. <https://doi.org/10.1590/S0100-40422011000300020>
  25. L. K. Shrestha, M. Thapa, R. G. Shrestha, S. Maji, R. R. Pradhananga, and K. Ariga, "Rice husk-derived high surface area nanoporous carbon materials with excellent iodine and methylene blue adsorption properties", *C-Journal of Carbon Research*, 2019, **5**(1), 10. <https://doi.org/10.3390/c5010010>
  26. S. Joshi, R. G. Shrestha, R. R. Pradhananga, K. Ariga, and L. K. Shrestha, "High surface area nanoporous activated carbons materials from *Areca catechu* nut with excellent iodine and



- methylene blue adsorption”, *C-Journal of Carbon Research*, 2021, **8**(1), 2.  
<https://doi.org/10.3390/c8010002>
27. B. Li, J. Hu, H. Xiong, and Y. Xiao, “Application and properties of microporous carbons activated by ZnCl<sub>2</sub>: adsorption behavior and activation mechanism”, *ACS omega*, 2020, 5(16), 9398-9407.  
<https://doi.org/10.1021/acsomega.0c00461>
28. J. Wang and S. Kaskel, “KOH activation of carbon-based materials for energy storage”, *Journal of materials chemistry*, 2012, **22**(45), 23710-23725.  
<https://doi.org/10.1039/c2jm34066f>
29. H. P. S. Abdul Khalil, M. Jawaid, P. Firoozian, U. Rashid, A. Islam, and H. M. Akil, “Activated carbon from various agricultural wastes by chemical activation with KOH: preparation and characterization”, *Journal of Biobased Materials and Bioenergy*, 2013, **7**(6), 708-714.  
<https://doi.org/10.1166/jbmb.2013.1379>
30. W., Chen, M., Gong, K., Li, M., Xia, Z., Chen, H., Xiao, ... & H., Chen, “Insight into KOH activation mechanism during biomass pyrolysis: Chemical reactions between O-containing groups and KOH”, *Applied Energy*, 2020, **278**, 115730.  
<https://doi.org/10.1016/j.apenergy.2020.115730>
31. Raymundo-Pinero, E., Azaïs, P., Cacciaguerra, T., Cazorla-Amorós, D., Linares-Solano, A., & Béguin, F. K. O. H., KOH and NaOH activation mechanisms of multiwalled carbon nanotubes with different structural organization, *Carbon*, 2005, **43**(4), 786-795.  
<https://doi.org/10.1016/j.carbon.2004.11.005>
32. M. M. Ghobashy and Z. I. Abdeen, “Radiation crosslinking of polyurethanes: characterization by FTIR, TGA, SEM, XRD, and Raman spectroscopy”, *Journal of Polymers*, 2016, **2016** (1), 9802514.  
<https://doi.org/10.1155/2016/9802514>
33. S., Rodiawan, and S. C. Wang, “The effect of impregnation ratio on the characteristics of activated carbon made from rubber fruit shells with KOH as the activation medium”, *IOP Conference Series: Earth and Environmental Science*, 2022, **1108**, (1), 012071.  
<https://doi.org/10.1088/1755-1315/1108/1/012071>
34. S. Bhunthong, D. Aussawasathien, K. Hrimchum, & S.N.Sriphalang, “Effects of Processing Parameters on Properties of Activated Carbon from Palm Shell: Sodium Hydroxide Impregnation”, *Chiang Mai Journal of Science*, 2017, **44**(2), 544-556.  
<http://epg.science.cmu.ac.th/ejournal/>